

Accepted Manuscript

The influence of low-temperature surface induction on evacuation, pump-out hole sealing and thermal performance of composite edge-sealed vacuum insulated glazing

Saim Memon, Yueping Fang, Philip C. Eames



PII: S0960-1481(18)31456-3

DOI: <https://doi.org/10.1016/j.renene.2018.12.025>

Reference: RENE 10900

To appear in: *Renewable Energy*

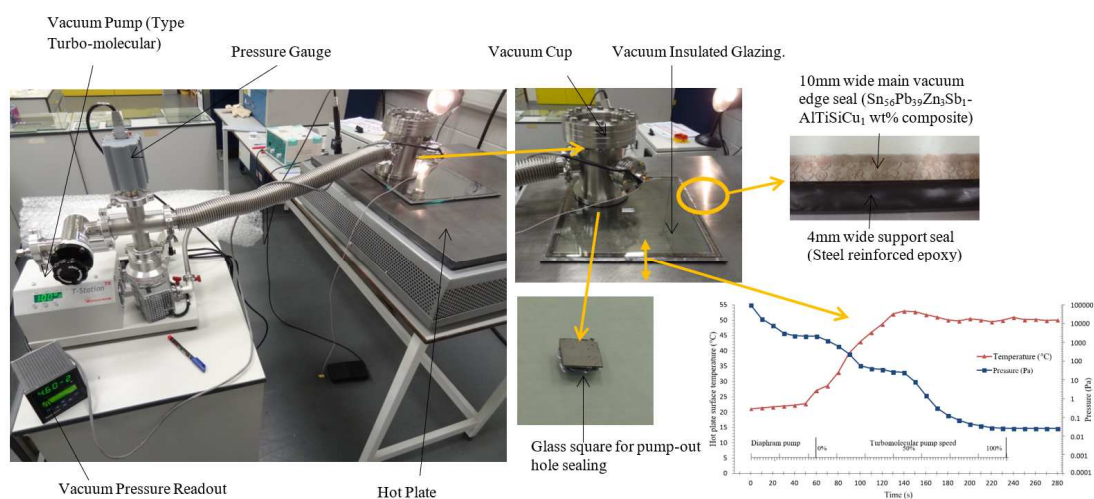
Received Date: 31 May 2018

Revised Date: 6 November 2018

Accepted Date: 6 December 2018

Please cite this article as: Memon S, Fang Y, Eames PC, The influence of low-temperature surface induction on evacuation, pump-out hole sealing and thermal performance of composite edge-sealed vacuum insulated glazing, *Renewable Energy* (2019), doi: <https://doi.org/10.1016/j.renene.2018.12.025>.

This is a PDF file of an unedited manuscript that has been accepted for publication. As a service to our customers we are providing this early version of the manuscript. The manuscript will undergo copyediting, typesetting, and review of the resulting proof before it is published in its final form. Please note that during the production process errors may be discovered which could affect the content, and all legal disclaimers that apply to the journal pertain.



The influence of low-temperature surface induction on evacuation, pump-out hole sealing and thermal performance of composite edge-sealed vacuum insulated glazing

Saim Memon^{13*}, Yueping Fang², Philip C. Eames³,

¹ London South Bank University, Centre for Advanced Materials, School of Engineering, 103 Borough Road, London, SE1 0AA, UK

² Coventry University · School of Energy, Construction and Environment, Priory Street, Coventry, CV1 5FB, UK

³ Centre for Renewable Energy Systems Technology (CREST), School of Mechanical, Electrical & Manufacturing Engineering, Loughborough University, Loughborough, Leicestershire, LE11 3TU, UK

*Corresponding Author: Saim Memon

Address: London South Bank University, Centre for Advanced Materials, School of Engineering, 103 Borough Road, London, SE1 0AA, UK

Email: S.Memon@lsbu.ac.uk

Tel: +44 (0)20 7815 7510

Abstract

Hermeticity of vacuum edge-sealing materials are one of the paramount requirements, specifically, to the evolution of energy-efficient smart windows and solar thermal evacuated flat plate collectors. This study reports the design, construction and performance of high-vacuum glazing fabrication system and vacuum insulated glazing (VIG). Experimental and theoretical investigations for the development of vacuum edgeseal made of Sn-Pb-Zn-Sb-AlTiSiCu composite in the proportion ratio of 56:39:3:1:1 by % (CS-186) are presented. Experimental investigations of the seven constructed VIG samples, each of size 300mm·300mm·4 mm, showed that increasing the hot-plate surface temperatures improved the cavity vacuum pressure whilst expediting the pump-out hole sealing process but also increases temperature induced stresses. Successful pump-out hole sealing process of VIG attained at the hot-plate set point temperature of 50°C and the approximate cavity pressure of 0.042 Pa was achieved. An experimentally and theoretically validated finite volume model (FVM) was utilised. The centre-of-pane and total thermal transmittance values are calculated to be $0.91 \text{ Wm}^{-2}\text{K}^{-1}$ and $1.05 \text{ Wm}^{-2}\text{K}^{-1}$, respectively for the VIG. FVM results predicted that by reducing the width of vacuum edge seal and emissivity of coatings the thermal performance of the VIG is improved.

Keywords: vacuum; glazing; solar-thermal; performance; modelling; transmittance

1. Introduction

Advancement in the vacuum sealing materials is one of the paramount need in leading smart windows [1] and solar thermal evacuated flat plate collectors [2] at the manufacturing level due to considerable issues of leakage in the vacuum edge sealing materials [3] and/or the cost of scarce semi-precious materials such as indium [4, 5]. There is also a serious challenge particularly in solar energy field of balancing the security of power supply and peak power demand [6]. Glazing technologies, such as double air-filled glazing [7] with low-e coatings [8] and gas filled glazing with cavities filled with heavy gases (Argon, Krypton or Xenon), could achieve the thermal transmittance value (U Value) up to $1.4 \text{ Wm}^{-2}\text{K}^{-1}$, depending on the cavity thickness [9, 10]. To improve the thermal performance further, without compromising the visible light transmittance, a vacuum insulation is an option. A vacuum insulation is a space, between two glass panes, of reduced mass of atmospheric-air. The rate of decrease of the density of air in a space determines the level of vacuum pressure. This provides thermal insulation, because with a lower density of air the mean free path between air molecules can be increased to above 1000 m [11], ultimately reduces the heat transfer path between air molecules in a space. In VIG, the space between two glass panes is evacuated to high-vacuum pressure (0.13 Pa to $1.33 \cdot 10^{-4} \text{ Pa}$) in order to reduce conductive and convective heat transfer [12] to negligible levels, however the heat transfer through radiation can only be minimised using low-emittance coatings to VIG [13]. In evacuated flat plate collectors, selective anti-reflective emissivity coatings onto the glass surface are required that improves optical transmission which is different to VIG in itself. Due to the difference between external atmospheric-air and internal vacuum pressure, spacers are required to prevent the glass panes touching each other [14]. These spacers are called support pillars and typically have radii from 0.1mm to 0.2 mm and height of 0.1mm to 0.2mm [15]. In VIG, even a small vacuum space gives the same thermal insulation because radiative heat transfer is same at any cavity thickness [16]. A vacuum edge seal around the periphery of the glass panes is required to maintain the high level of vacuum and avoid the problems of gas leaks, degradation of coatings, and absorption of moisture. However, heat transfer through conduction occurs because of the contiguous heat transfer path formed by the support pillar and edge sealing materials.

The constructional components that mainly determines the thermal performance of VIG is its vacuum edge seal [17,18]. The vacuum edge seal of a VIG must be capable of maintaining a vacuum pressure of less than 0.1 Pa [19], in order to suppress gaseous conduction, for the expected life of 20 years. The edge of two glass panes was first sealed using a high power laser through a quartz window in a vacuum chamber [20] but the level of vacuum was not less than the required, 0.1 Pa, due to gases and vapour molecules caused by laser sealing technique [21, 22]. A high-temperature edge sealing material, Schott solder glass type 8467 at the sealing temperature of 450°C , was used by the group at the University of Sydney [12, 23, 24]. With this technique, it achieved centre-of-pane thermal transmittance (U_{centre}) value of $0.8 \text{ Wm}^{-2}\text{K}^{-1}$ and subsequently developed to the production level under the trade name of 'SPACIA' in Japan by Nippon Sheet Glass (NSG) [25]. The problems with the high-temperature edge sealing method is that it causes degradation of soft low emittance coatings meaning that only hard coatings can be used [13]. Toughened glass also cannot be used due to the loss of temper at high temperatures [26]. Low-temperature solder glass materials were investigated to form a hermetic edge seal, but durability was a problem due to the absorption of moisture. Polymers have problems of both gas permeability and out gassing [4, 27]. A low-temperature edge sealing materials, i.e. indium or indium alloys melts at about 160°C , were utilised and developed at the University of Ulster [13, 28, 29]. This technique achieved a U_{centre} value of $0.9 \text{ Wm}^{-2}\text{K}^{-1}$

and allowed the use of low emittance soft coatings (such as silver), which reduce radiative heat transfer between the glass panes and permits toughened glass pane for an increase of support pillar spacing that reduces conductive heat transfer. The problems with the low-temperature based indium seal are the scarcity and the cost; because of this, the low-temperature indium sealed vacuum glazing process has not yet been commercialised [4,9, 30].

In this paper, a particular focus is made on the design and construction of high-vacuum glazing fabrication system, including the modified vacuum cup, and a new method of vacuum edge seal utilised for the successful fabrication of the VIG, made of Sn-Pb-Zn-Sb-AlTiSiCu composite in the proportion ratio of 56:39:3:1:1 by % weight respectively, developed by MBR Electronics GmbH in the trade name of CS-186. A steel reinforced epoxy applied to support the vacuum edge seal, as illustrated in Fig. 1. One of the significant contribution in this paper is reporting the experimental investigations of seven VIG samples for evaluating the influences of hot-plate surface temperatures induction on evacuation and pump-out hole vacuum sealing of the VIG in order to achieve the relatively acceptable setup when the evacuation and pump-out hole sealing processes are performed. An experimentally and theoretically validated finite volume model (FVM) of Fang et al.(2005) [31]; Fang et al.(2006) [15] and Fang et al. (2009) [22] was utilised for the thermal performance analyses of VIG, size of 300mm·300mm·4mm rebated by 10 mm in a solid wood frame and 10 mm main edge seal and the results are discussed.

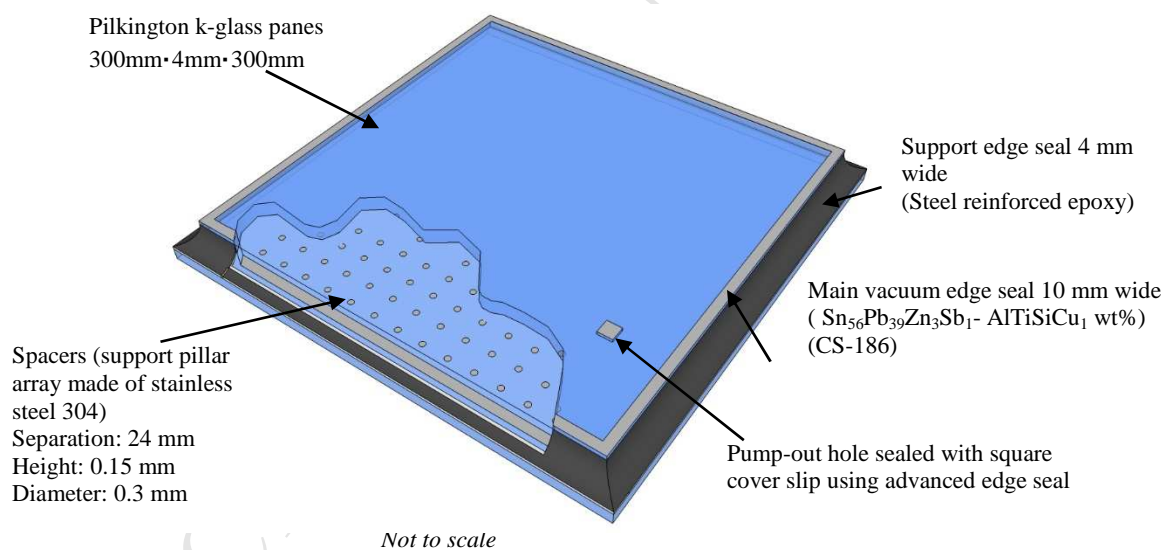


Fig. 1. A schematic diagram of novel edge sealed VIG showing the main vacuum edge seal 10 mm wide, made of Sn-Pb-Zn-Sb-AlTiSiCu composite in the proportion ratio of 56:39:3:1:1 by wt% respectively) (CS-186), and a support edge seal 4 mm wide, made of steel reinforced epoxy.

2. Design and construction of a high-vacuum glazing fabrication system

A lab scale vacuum glazing fabrication system was designed and constructed to fabricate VIG. The vacuum glazing production system design, as shown in Fig. 2, consists of the vacuum pump, it is connected in series with the vacuum cup. For the measurement of pressure, a pressure gauge is connected in parallel with the vacuum pump. The angle valve with Swagelok adapter is included allowing the system to be purged with nitrogen (inert gas); this is connected in series with a square cross-section tube. An angle valve

is connected in series between the vacuum pump and vacuum cup. The dimensions of the components used in this design are presented in Table 1. A dry type turbo-molecular with backing pump with an achievable pressure of $5 \cdot 10^{-6}$ Pa was chosen. This is because the vacuum pump should be of an oil free/dry type as the contamination in the oil type with oil molecules could occur on the surfaces of tubes, valves, hose and/or vacuum cup preventing an achievement of effective vacuum level. A turbo-molecular vacuum pump has a pumping speed of 61 litres/sec. With proper venting, the turbo mechanism stops in less than a minute. This means that vacuum cup venting is accomplished without the need for a valve to separate the pump and vacuum cup. The EXT75DX T-Station selected for this vacuum system. It consists of a turbo molecular pump and a diaphragm-backing pump XDD1. The ATV (Atmosphere to Vacuum) transducer type 979, was connected to a PDR 900 digital pressure measurement readout, used in the present study for the measurement of vacuum pressure in the designed vacuum system. This pressure gauge is located at the closest possible location to the vacuum cup to measure the approximate pressure in the cavity of the VIG, as shown in Fig. 2. The ATV transducer enables measurement of a wide pressure range from ultrahigh vacuum ($1.33 \cdot 10^{-8}$ Pa) to atmospheric pressure ($101.33 \cdot 10^3$ Pa). It consists of MEMS (Micro-Electro-Mechanical System) based MicroPirani gauge and a miniaturised hot cathode ionisation gauge in a single transducer unit [32]. The MEMS based MicroPirani gauge measures pressure from $1.33 \cdot 10^{-2}$ Pa to atmospheric pressure. The hot cathode ionisation gauge measures pressure from $1.33 \cdot 10^{-3}$ Pa down to $1.33 \cdot 10^{-8}$ Pa. A good discussion and literature review of the fundamental theory of Pirani and hot cathode ionisation gauges can be found in text books by Dennis and Heppell (1968) [33] and Guthrie (1963) [34]. The PDR900 digital controller provides readout of the pressure measurements. It interfaced to a computer for real time data logging of the evacuation pressure of the vacuum system.

Table 1

Dimensions of the components used in the vacuum system design.

Components	D (cm)	L (cm)	V (cm ³)
Angle valve with Swagelok adapter	$D_3=4.2$	$L_3=11$	152.4
	$D_4=3.8$	$L_4=4.7$	53.3
	$D_5=3.8$	$L_5=4.7$	53.3
Square cross-section tube	$D_1=3.8$	$L_1=4.1$	46.5
	$D_2=3.8$	$L_2=4.1$	46.5
	$D_6=3.8$	$L_6=4.1$	46.5
	$D_7=3.8$	$L_7=4.1$	46.5
Angle valve	$D_8=4.2$	$L_8=11$	152.4
	$D_9=3.8$	$L_9=4.7$	53.3
	$D_{10}=3.8$	$L_{10}=4.7$	53.3
hose/pipe	$D_{11}=3.8$	$L_{11}=69$	782.54
Vacuum cup	$D_{12}=3.5$	$L_{12}=2$	1.1
	$D_{13}=10$	$L_{13}=15$	23.56
	$D_{14}=3.5$	$L_{14}=2$	1.1
	$D_{15}=3.5$	$L_{15}=2$	1.1

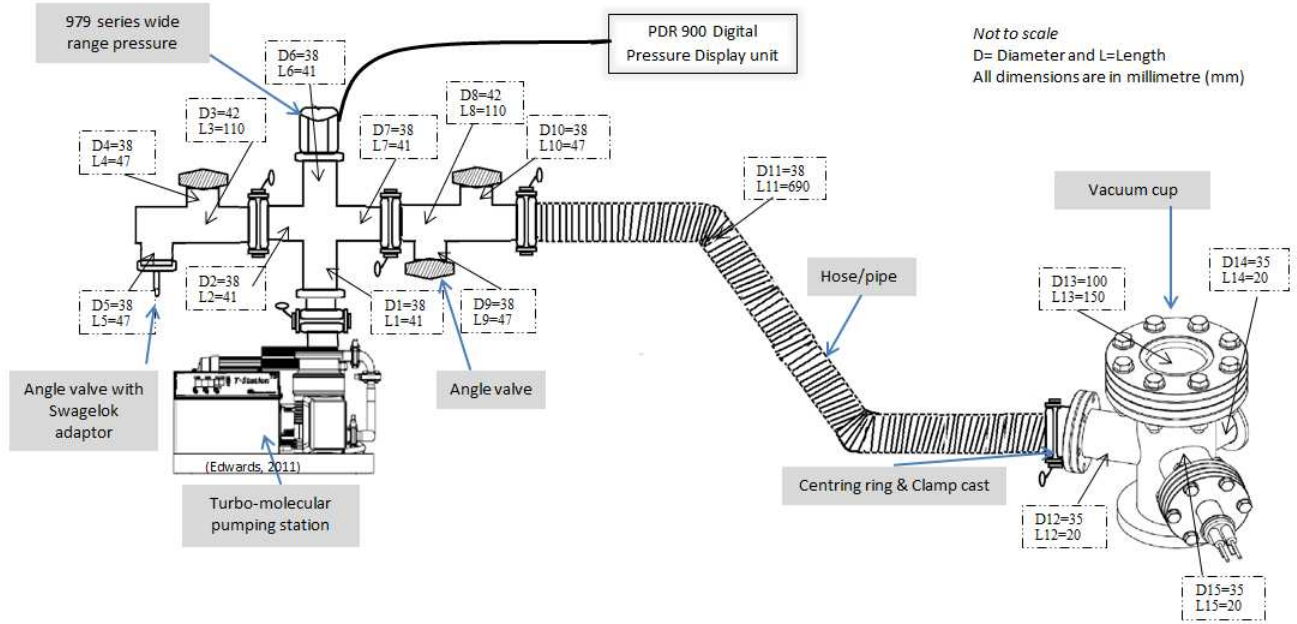


Fig. 2. A schematic diagram of the designed vacuum system showing the dimensions and connections of the tubes, angle valves, the vacuum cup and the vacuum pump.

To obtain a vacuum in a volume of the system the density of gas must be reduced and is directly proportional to the gas pressure; in practice, the gas pressure measures the level of vacuum [35]. The rate at which the gas molecules are evacuated from the vacuum vessel, i.e. mass flow, determines the pressure drop. The mass flow rate, M , can be expressed (in atomic mass unit of gas) by keeping the mass of gas, m , and temperature, T , in the vessel constant as Eq. (1),

$$\frac{dM}{dt} = \frac{m}{\zeta T} Q \quad (1)$$

Where ζ is the Boltzmann constant i.e. $1.38 \cdot 10^{-23} \text{ Pa m}^2 \text{ K}^{-1}$ and Q is the gas flow rate in Pa litres/sec. This can be expressed by knowing the pressure, P , and volume, V , of the gas as Eq. (2),

$$Q = \frac{d(PV)}{dt} \quad (2)$$

The gas flow, Q , through a vacuum vessel or hose occurs due to the difference of pressure depending on the inside diameter of the tubes. The average distance any air molecule travels before colliding with another molecule is its mean free path λ in m [34, 36]. The collisions between molecules can be calculated using Eq. (3).

$$\lambda = \frac{\zeta T}{\sqrt{2} \pi P D_m^2} \quad (3)$$

Where, T is the absolute temperature of the air in K (the tubes are under atmospheric air with an ambient temperature of 294.15K) and P is the air pressure in Pa. D_m is the gas kinematic diameter of the air molecule i.e. $4 \cdot 10^{-10} \text{ m}$, which is based on the assumption that the air molecules are smooth, rigid and elastic spheres [37].

The turbo-molecular pump evacuated the air molecules continuously from the tubes, components, vacuum cup and cavity of the VIG. The rate at which the volumetric flow of gases evacuated from the system is the pumping speed in litres/sec, in this type of turbo-molecular pump the ultimate pumping speed is given to be 61 litres/sec. One of the considerations was taken into account when designing the vacuum system was to reduce the connections (tubes and pipe length) between the turbo-molecular pump and the vacuum cup so as to keep the pumping speed losses to a minimum level.

Upon initiating a pump down the flow of air molecules, having air pressure of 101.325 kPa, was often turbulent, called viscous flow regime. In which the mean free path between molecules was calculated to be $56.35 \cdot 10^{-9}$ m from the Eq. (3). As the air pressure decreases the mean free path increases, having a fewer air molecules in a space to make collisions with each other and the mean free path is considered to be roughly equivalent to the diameter of the tube, called a laminar (transition) flow regime. In a best-case scenario, when the achievable vacuum pressure is $5 \cdot 10^{-6}$ Pa then the mean free path between molecules is calculated to be 1142 m, called a molecular flow regime.

The rate of evacuation, i.e. gas flow rate, is proportional to the rate of mass of air change. In addition to that, the layers of adsorbed gaseous molecules as a thin film on the internal surfaces within the tubes and vacuum glazing require evacuation of six hours to achieve a good level of high vacuum pressure. Increasing the temperature from 100°C could help in desorbing the layers of gaseous molecules but this may cause glass bending. This increases internal compressive and external tensile stresses in the glass panes and increases the risk of cracking of the edge seal. With a constant temperature, up to 60°C, and volume of the vacuum system the flow rate into the turbo-molecular pump (Q_i) from the vacuum system can be written as Eq. (4),

$$Q_i = S_o P_v \quad (4)$$

The flow rate into the turbo-molecular pump (Q_i) can be calculated to be $3.05 \cdot 10^{-4}$ Pa litres/sec from the S_o ultimate pumping speed i.e. 61 litres/sec and the P_v ultimate pump pressure i.e. $5 \cdot 10^{-6}$ Pa.

A high-vacuum glazing fabrication system constructed is shown in Fig. 3. It is based on the design presented in Fig. 2. The vacuum system was experimentally tested and the minimum achievable vacuum pressure was recorded to be $4.35 \cdot 10^{-5}$ Pa. This deviates by 7.7% with the ultimate vacuum pressure of the turbo molecular pump due to tube air-flow conductances.

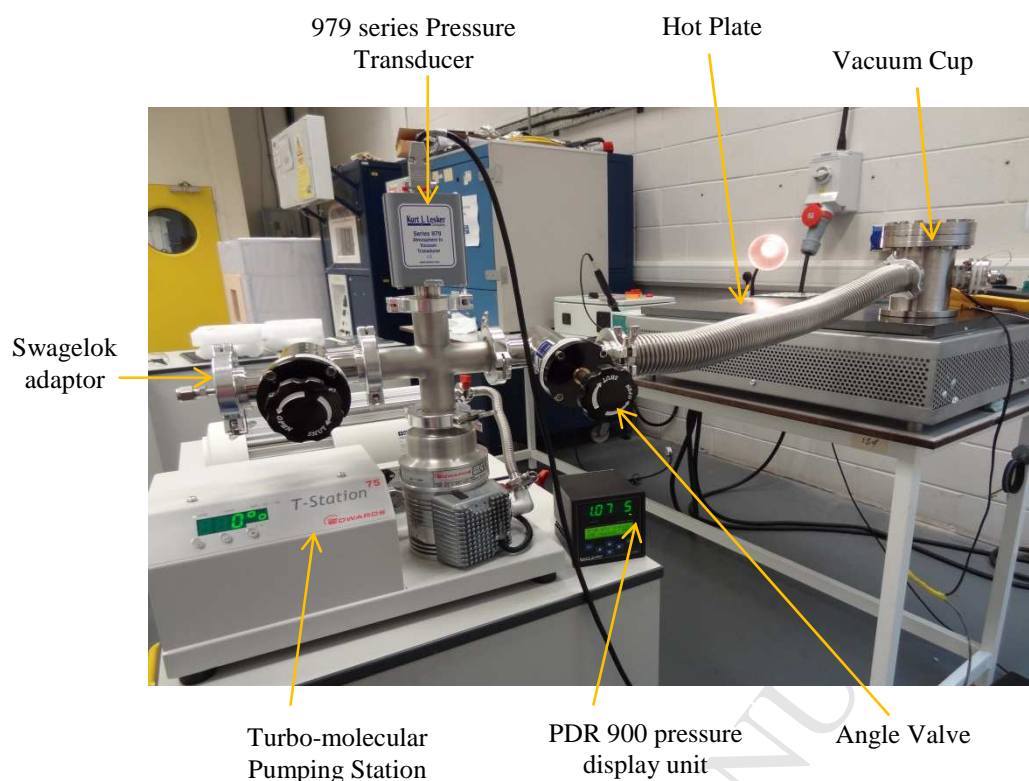


Fig. 3. A photograph of the vacuum system developed based on the design presented in Fig. 2.

2.1. Vacuum Cup for Pump-out hole sealing during Evacuation

A number of vacuum cup designs were used in previous studies for the evacuation and sealing of the pump-out hole of a vacuum insulated glazing. The first successful method of pump-out hole sealing was based on sealing a capillary glass tube [12, 25]. The capillary tube was bonded to the pump-out hole using solder glass during the edge sealing process and was then sealed after evacuation. An electrical resistance heater mounted inside a vacuum cup and looped around the capillary tube. Resistance heating permits the tube to be sealed at around 600°C when the correct vacuum was achieved. A modified pump-out sealing technique was reported by Zhao et al. (2007) [28], this approach has used low-temperature indium alloy soldered ultrasonically on to a glass disc for pump-out hole sealing and a cartridge heating element fixed inside a steel block in the pump-out cap to melt the indium and seal the hole. This method was found to be difficult in positioning the glass disc over the pump-out hole with a risk of dislocation of the heating block when the indium alloy on the glass disc melted during evacuation. In this paper, a new vacuum cup design is presented for the evacuation and vacuum sealing, suitable for both high-temperature and low-temperature materials, of the pump-out hole on the VIG, as illustrated schematically in Fig.4. In this design, the risks of dislocation and degradation of O ring (to avoid ingress of gas molecules from the atmosphere) were minimised to a negligible level by: (i) designing the vacuum cup diameter of 100 mm to make the Viton O ring sufficiently away from the heating element to avoid degradation, which is capable of sustaining temperatures up to 250°C; and (ii) the heating element (cartridge heater) and K type thermocouple are mounted to a metallic rod controlled through a supporting Y shaped block to provide vertical motion of up to 10 mm, as shown in Fig. 5(a). A K type thermocouple fixed to the heating block measures the approximate pump-out hole seal, made of glass square, temperature as shown in Fig 5(c). Heat transfer at high vacuum occurs through both long wave radiation and conduction due to contact between the heating block and the glass disc, as shown in Fig 5(b) and Fig 5(d). The required temperature to achieve a vacuum

pump-out hole seal is approximately 40°C greater than the melting temperature of the pump-out sealing material used to seal the pump-out hole.

Fig. 4 also shows the pump-out hole on top of the VIG located inside the vacuum cup. The radius of the pump-out hole on the top glass pane was reduced to less than 1.5mm in order to minimise the use of pump-out sealing material. To reduce the risk of glass fracture and risk of scratches on the glass surface due to manual drilling, a glass drilling machine at a local glass pane supplier was used for pump-out hole drilling. However, due to the limitations in the available drill radius, the minimum possible pump-out hole radius and volume was 2 mm and 50.26 mm³, respectively, were chosen. The volume of the vacuum gap in the VIG (area of 280·280 mm, subtracted the area of edge seal), shown in Fig. 4, was calculated to be 11758.47mm³ (0.012litres) by taking into account the total number of pillars and volume occupied in a vacuum gap that are 144 (a pillar spacing of 24mm) and 1.53mm³, respectively. Thus, the total volume including the vacuum system was calculated to be 1.52 litres. The total volume of the system is considered to be sufficient for the evacuation of vacuum insulated glazing due to the high pumping speed of the selected turbo molecular pump i.e.61 litres/sec.

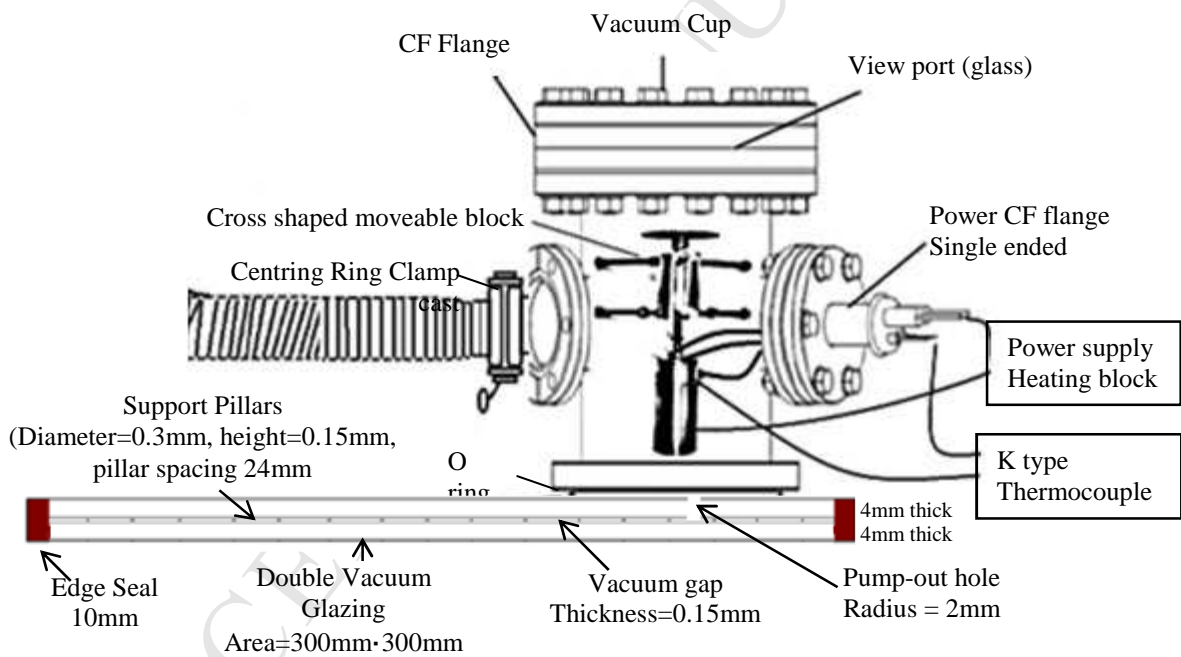


Fig. 4. A schematic diagram of the vacuum cup design showing the heating block used for sealing the pump-out hole on the VIG.

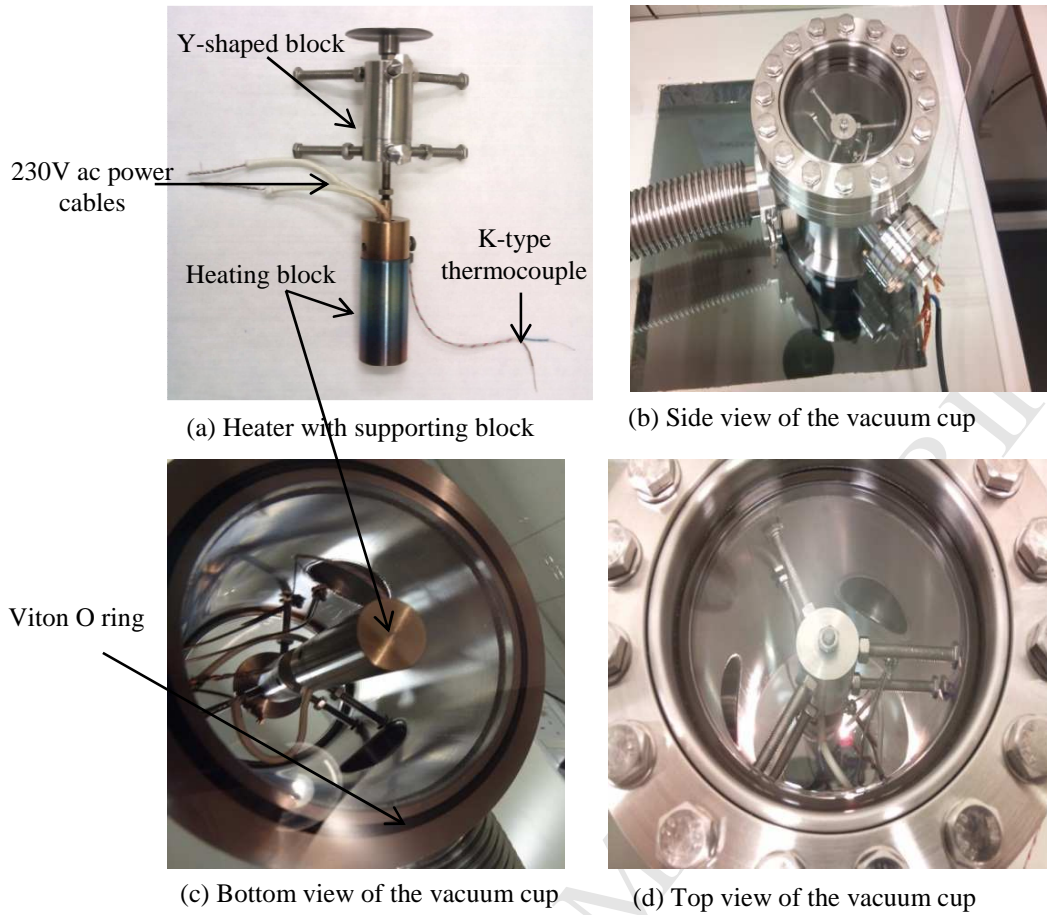
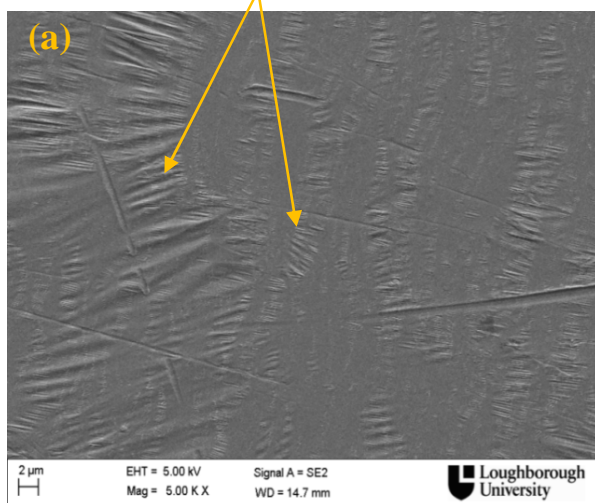


Fig. 5. Illustrations of the constructed vacuum cup system for the evacuation and sealing of the pump-out hole in a VIG.

3. FIB-SEM and X-ray CT analysis of CS-186 composite (vacuum edge seal)

Focus Ion Beam Scanning Electron Microscopic (FIB-SEM) and X-ray high resolution Computed Tomographic (CT) systems were used to analyse the micro-structural surface of the main edge seal's smoothness and consistency of CS-186 composite. In the first part, a cover slip, size of 20mm·20mm·1mm, ultrasonically soldered with CS-186 composite. In the second part, two Pilkington K glass panes, each of size 10mm·10mm·4 mm, ultrasonically soldered CS-186 composite and then heated at 186°C in a radiative oven. Fig. 6(a) shows the smooth and consistent flow of the spread of this composite onto the glass surface. It was found that the continuity of the composite-soldered layer on to the glass edges determines the integrity of the seal. Fig. 6(b) shows the cross-sectional views of the interface between the glass to CS-186 composite. As it can be seen, the cross-sectional middle view of the glass- CS-186 composite seal has negligible traces of micro voids with trapped air inside, this determines the hermeticity and the contiguity of the edge seal when used for the construction of VIG. Although the trapped air inside the edge seal is one of the common issue in the formation of the edge seal as examined by Zhao et al (2007) [28]. This can greatly be reduced by applying carefully the ultrasonic soldering iron at the vibration frequency of 25-30 kHz with the set-point temperature of 190°C (the melting temperature of this composite is 186°C). Overheating must be avoided [13, 21] and a secondary support seal is necessary to avoid the risk of external mechanical stresses due to manual handling of the VIG sample.

Multiple straight-lines caused by the ultrasonic soldering iron at 25 kHz necessary as part of the formation of edge



Pinholes with air trapped inside

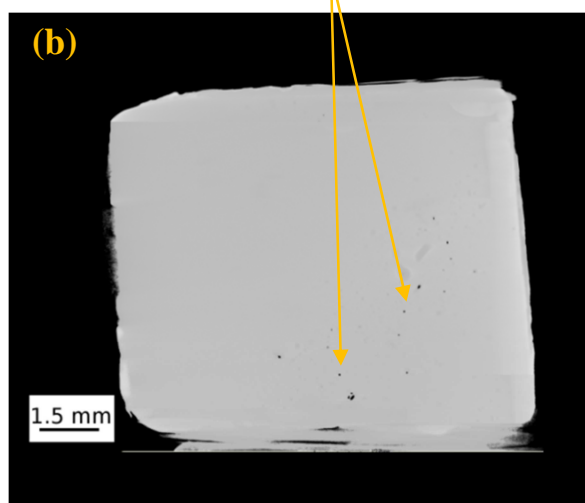


Fig. 6. (a) FIB-SEM of 20mm·20mm·1mm slide cover slip sample with $\text{Sn}_{56}\text{Pb}_{39}\text{Zn}_3\text{Sb}_1\text{-AlTiSiCu}_1$ wt% composite (also called CS-186 composite) ultrasonically soldered on the surface magnified at 5000x (b) X-ray CT cross-sectional view at the interface of the glass and CS-186 composite seal.

4. Design and construction of the VIG

4.1. Four-stage design process

The four-stage design process for the construction of vacuum edge seal is developed, as shown in Fig. 7, using the high-vacuum pump-out system. Two 4 mm thick Pilkington K-glass panes of area 292mm·292mm (upper glass) and 300mm·300mm (lower glass) were used. The reason for using different sizes of glass panes was to apply support edge seal (steel reinforced epoxy) uniformly around the periphery of the VIG to support the main edge seal made of $\text{Sn}_{56}\text{Pb}_{39}\text{Zn}_3\text{Sb}_1\text{-AlTiSiCu}_1$ wt% (CS-186) composite. The width of the primary edge seal was considered to be constant i.e. 10 mm and a support edge seal i.e. 4mm to test and repeat the experiments for the successful fabrication of VIG based on this new method. A selection of 10 mm width of the edge seal was the result of experiments performed to increase the mechanical stability of the main edge seal. The process achieved after rigorous experiments is detailed section 4.2.

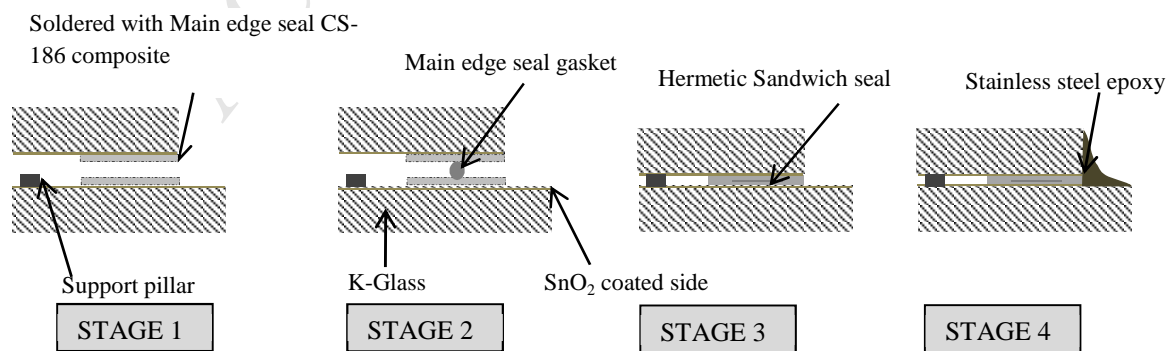


Fig. 7. Four stage design process for the construction of vacuum edge seal.

4.2. Construction process

1) 4 mm thick K-glass panes were cut to the size of 292mm·292mm and 300·300mm. In the smaller pane, a 4 mm diameter of pump-out hole drilled to allow the evacuation of the cavity between the two glass panes, located 75 mm from the corner of the smaller glass pane.

2) The panes of glass were cleaned with water, acetone and isopropanol followed by an initial bake-out at 120°C in an oven.

3) A 10 mm wide layer of CS-186 composite was ultrasonically soldered around the periphery on the SnO₂ coated sides of both glass panes in the arrangement, as shown in the Fig. 8. Subsequently, a square cover slip of 1mm thick cutting to a size of 18·18mm was prepared for the pump-out hole sealing by soldering with CS-186 composite.

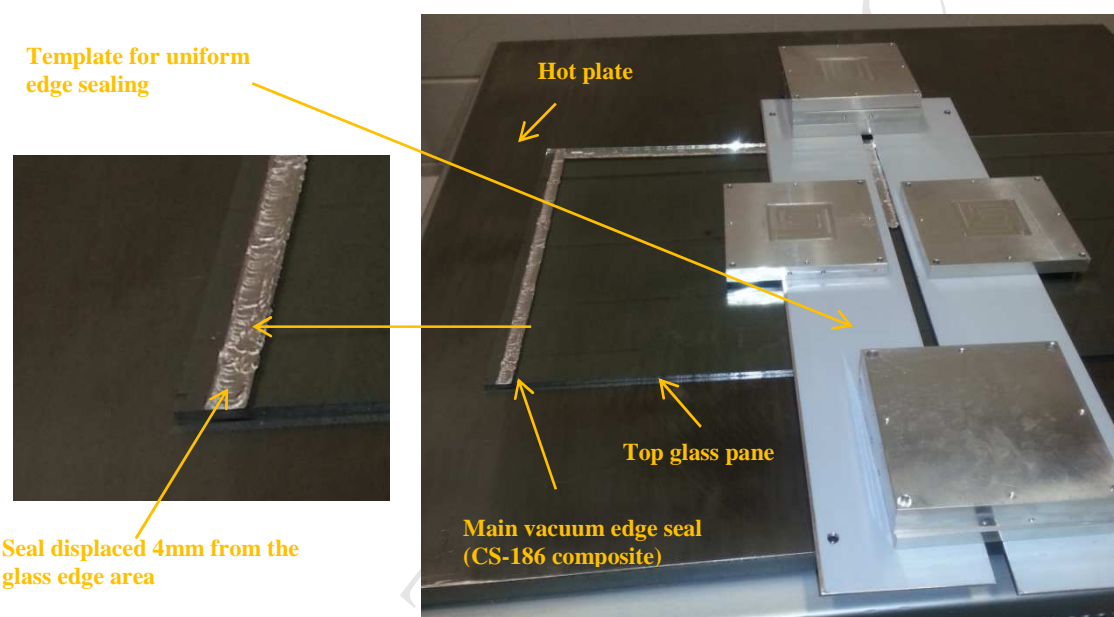


Fig. 8. The 10 mm wide primary seal soldered on the bottom glass pane around the periphery, displaced 4mm from the glass edge.

4) Stainless steel support pillars were located on the lower glass pane using a vacuum wand as illustrated in Fig. 9a. The pre-soldered upper glass pane was located on top of the support pillars.

5) A CS-186 composite wire gasket was placed on the soldered area as illustrated in the Fig. 9b.

6) The prepared sample, shown in Fig. 9c, was heated to 186°C in the oven to join two panes of glass together for up to 2 hours.

7) A support seal, steel reinforced epoxy, was applied around the edges of the main edge seal for enhancing the mechanical stability of the main edge seal, as shown in the Fig. 9d.

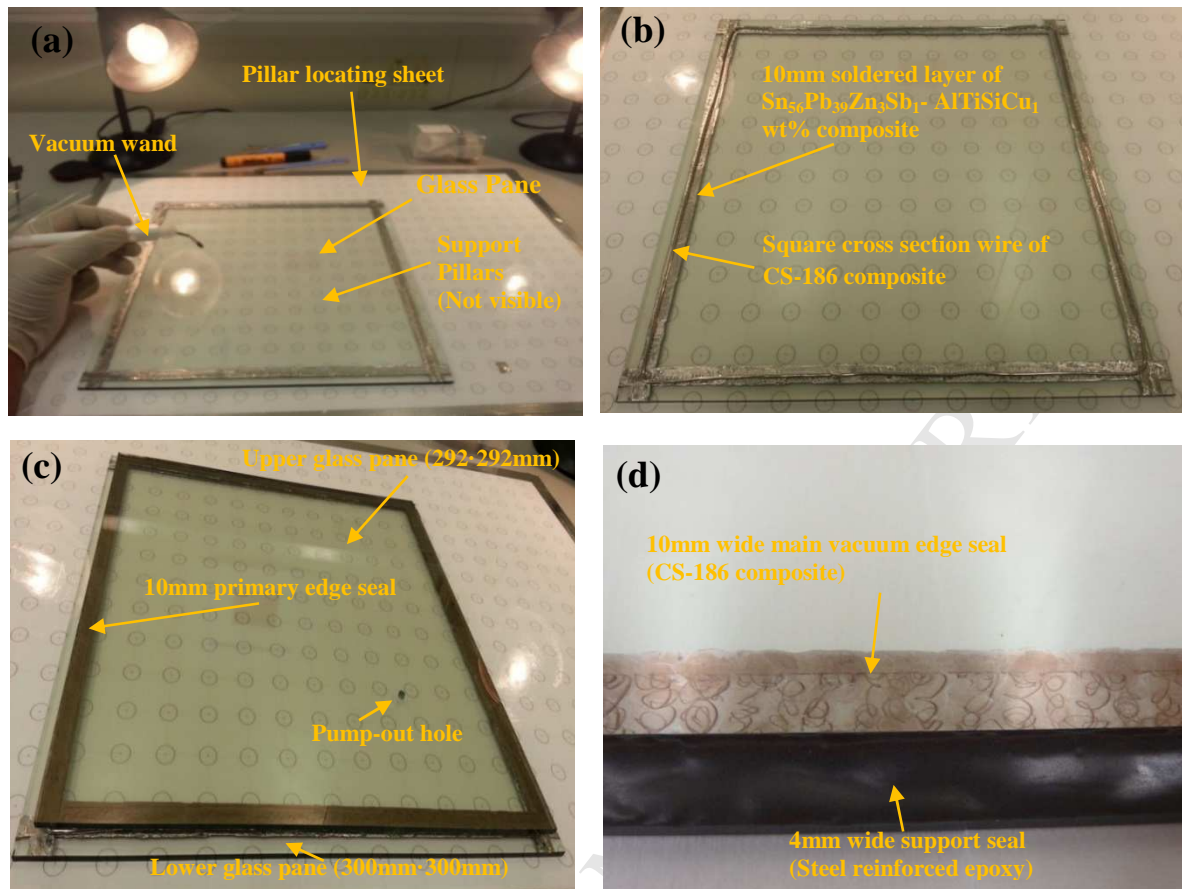


Fig. 9. shows (a) support pillars placing on the lower glass pane using a vacuum wand, (b) the square cross section wire made of the $\text{Sn}_{56}\text{Pb}_{39}\text{Zn}_3\text{Sb}_1\text{-AlTiSiCu}_1$ wt% composite (also called CS-186) 1.6mm in diameter placed on the soldered main edge seal to form a gasket, (c) the prepared sample before heating in the oven to 186°C illustrates the upper glass pane (292mm·292mm) placed on the lower glass pane (300mm·300mm) separated by the edge seal and an array of support pillars, and (d) the edge seal made of CS-186 composite and steel reinforced epoxy around the periphery of the sample.

8) The sample was then placed on the hot plate and heated to variable temperatures for improving evacuation of the cavity in the sample using the vacuum cup connected to the high-vacuum pump-out system.

9) During evacuation, after 6 hours, the pump-out hole was sealed by heating the CS-186 composite coated glass square using the cartridge heater fixed inside the vacuum cup as illustrated in the Fig. 10.

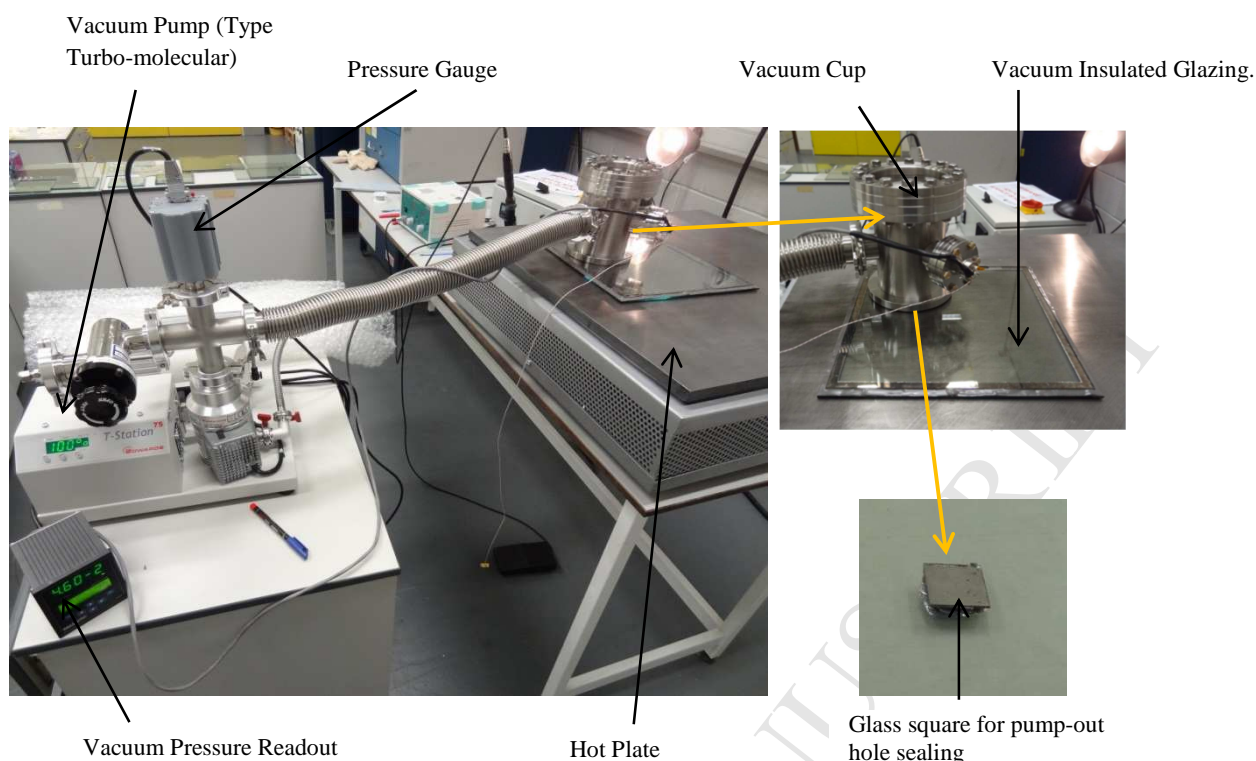
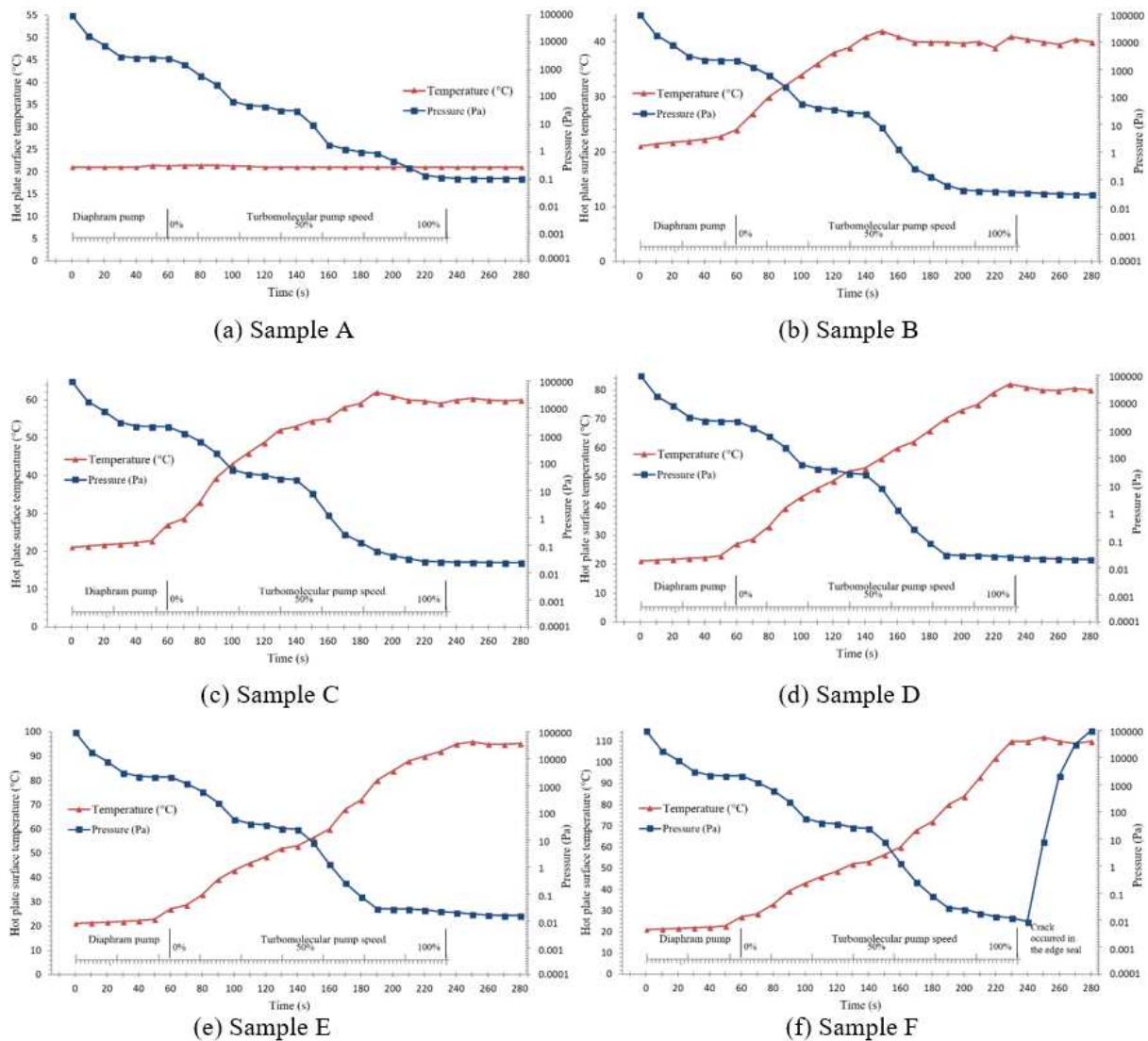


Fig. 10. Experimental setup developed for the evacuation of VIG using a vacuum cup connected to a vacuum system and the pump-out hole sealed with a glass square.

5. Influences of surface temperatures induction on evacuation and pump-out hole sealing of VIG

An ability of VIG to withstand the mechanical stresses is contingent to the strength of the panes of glass and the edge seal. These are the characteristic attributes inherent to the consistent formation of the whole sample, when the cavity vacuum pressure of less than 0.1 Pa and the pump-out hole seal are achieved. Due to the mutual external and internal forces of such a complex procedure, keeping the concentration of the stresses around the pump-out hole area and keeping the minimum possible deflections of the glass surfaces are significant factors in achieving the successful VIG unit. It is important to mention here that uniform temperature distribution and cooling at a slower rate [38] must be introduced because of the thermal expansion mismatch between the glass pane and the main edge seal, i.e. $8 \cdot 10^{-6}/^{\circ}\text{C}$ and $23.5 \cdot 10^{-6}/^{\circ}\text{C}$ respectively. In this paper, the novel contribution is not only to fabricate VIG but to achieve the prominent vacuum pressure and sustainable surface temperatures with the minimum possible additional stresses. The hot-plate surface temperature and approximate cavity pressure measurements varying with time were performed simultaneously on the seven samples fabricated, each was 300mm·300mm·4mm in size made of K glass. These samples were sealed, around the periphery of the two glass panes, with the main edge seal 10 mm wide made of $\text{Sn}_{56}\text{Pb}_{39}\text{Zn}_3\text{Sb}_1\text{-AlTiSiCu}_1$ wt% composite, and a support edge seal, 4 mm wide, made of steel reinforced epoxy. The hot-plate surface temperatures, reported here, were as measured for each sample and for each measurement the temperature controller was set to the appropriate value to study experimentally the influence of hot-plate surface temperatures on the evacuation of the cavity pressure and the pump-out hole sealing of the VIG for the purpose of achieving the viable high-vacuum pressure with the minimum possible stresses. Such stresses are because of shear forces occurred on the edge seal area forcing the glass into curve relative to the centre-of-pane surface. Both glass panes deflect, under the

1 induction of temperature differentials, in the same direction that are usually caused during the evacuation
2 and pump-out hole sealing process.



3 Fig. 11. Experimental measurements of hot-plate surface temperature induction and vacuum pressure regimes in
4 which: (a) Sample A at the set-point of 21°C achieved 0.1 Pa; (b) Sample B at the set point of 40°C achieved 0.05 Pa;
5 (c) Sample C at the set point of 60°C achieved 0.04 Pa; (d) Sample D at the set point of 80°C achieved 0.03 Pa; (e)
6 Sample E at the set point of 95°C achieved 0.02 Pa; and (f) Sample F at the set point of 110°C achieved 0.009 Pa.
7

8 Fig. 11a shows the experimental measurements of the approximate cavity pressure under the ambient
9 temperature of 21°C. As can be seen, the vacuum pressure of approximately 0.1 Pa was achieved during the
10 evacuation. The glass square was heated, using the heating element inside the vacuum cup, gradually to the
11 melting temperature of this composite, i.e. 186°C, during evacuation. Due to the temperature gradients on
12 the glass panes, the sample-A has experienced increasing level of internal compressive and external tensile
13 stresses. This results a small crack on the upper glass around the pump-out hole sealing area occurred after
14 10 min during evacuation. It was noticed that that the sample-A must be subjected to an appropriate surface
15 temperatures by making sure the surface temperature must not degrade the edge seal. These experimental
16 results are in good agreement with the detailed mathematical model and calculations of the predicted
17 temperature induced stresses reported by Collins et al. (1992) [24], Fischer-Cripps et al. (1995) [14],
18 Lenzen and Collins (1997) [39], Wang et al. (2007) [21] and Wullschlegel et al. (2009) [40].

The Sample-B was fabricated, as shown in Fig. 11b, showing the experimental measurements of the approximate cavity pressure of 0.05 Pa at the set-point hot-plate surface temperature of 40°C. The pump-out hole of the Sample-B was sealed with glass square but it experienced a small leak, after 15 min of evacuation, on the pump-out hole seal due to the insufficient temperature distribution. However, it can also be seen that the vacuum pressure was improved as a result of increasing the Sample-B hot-plate surface temperature but a proper temperature gradient match was needed between the top-glass surface and the heating block inside the vacuum cup. Subsequent stresses observed are tensile on top glass pane and higher compressive on bottom glass pane as predicted by Wang et al. (2007) [21].

Fig. 11c shows the Sample-C temperature/pressure profiles in which the experimental measurements of the improved approximate cavity pressure of 0.04 Pa at the set-point hot-plate surface temperature of 60°C were recorded. The Pump-out hole of the Sample-C was successfully sealed with glass square after 6 hours of evacuation. This is because the layers of adsorbed gaseous molecules as a thin film on the internal surfaces within the tubes and vacuum glazing require longer evacuation. The evacuation process time can be reduced by increasing the surface temperatures.

To further improve the approximate cavity pressure, Sample-D was fabricated in which the approximate cavity pressure of 0.03 Pa at the set-point hot-plate surface temperature of 80°C were recorded, as shown in Fig. 11d. During the pump-out hole sealing process, it was observed that the Sample-D experienced tensile stresses on the top pane whilst compressive on the bottom pane causing glass bending and fractured the sample from its edges after 1.5 hours of evacuation during the formation of the pump-out hole seal.

Such initial experimental investigations show when the hot-plate surface temperature was set to 21°C then it caused difficulty in the formation of pump-out hole seal leading to the growth of crack on the top glass pane. An increase of hot-plate surface temperature facilitates the sealing of the pump-out hole, whilst achieving improved vacuum pressure, but increases the stresses causing bending of the glass panes and produces a risk of fracture to the edge seal. Although the uniform glass surface temperatures are practically not possible due to the limitations of the edge seal temperature for the formation and the mechanical sensitivity of the main edge seal despite the fact the coefficient of thermal expansion of the glass and the edge seal are within their acceptable margins.

Fig. 11e shows the temperature/pressure measurements of Sample-E in which the approximate cavity pressure of 0.02 Pa, at the set-point hot-plate surface temperature of 95°C, was achieved. The pump-out hole of the sample-E was successfully sealed but it experienced higher level of internal compressive and external tensile stresses, after 20 min of evacuation, caused the fracture of the edge seal.

To comprehend the limitation of the VIG sample surface temperatures and its maximum achievable vacuum pressure, Sample-F was fabricated in which the approximate cavity pressure of 0.009 Pa at the set point temperature of 110°C were recorded, as shown in Fig. 11f, but cracks occurred, after 4 min of evacuation, on to the edge and the pump-out hole areas. It is because of the glass bends due to thermal stresses and higher temperature differentials fractured the glass. However, the vacuum pressure was improved before 4 min of evacuation by increasing the sample temperature but it also increased the stresses, glass deflections, and caused difficulties in sealing the pump-out hole.

A relatively acceptable, based on the aforementioned experimental observations, an improved VIG sample was made at the hot-plate set-point temperature of 50°C, as shown in the Fig. 12. The approximate cavity pressure of 0.042 Pa was achieved and the hot-plate surface temperature and pressure regimes were recorded as shown in Fig. 13. It was fabricated after a series of six experiments. In which the influence of hot-plate surface temperatures on the cavity vacuum pressures and their limitations were experimentally studied. A practicable fabrication process was achieved from these experiments and effective sample successively constructed. More than five similar samples of this process having different sizes, re-evacuated at the hot-plate set-point temperature of 50°C, were fabricated which validates the recurrent sealing of the pump-out hole and achievable vacuum pressure. The experimental observations show repetitive behaviour of stress patterns across the support pillars indicated a vacuum-tight edge seal, as shown in Fig. 12. A new contribution to this study is that the temperature induces not only stress but it also improves vacuum pressure and achieving the match of hot-plate surface temperature of 50°C for this type of edge seal was a prominent challenge in this study and contribution to the VIG sample. However, the preceding studies have already reported the mathematical modelling of the stresses in vacuum glazing and in this paper the repetition was avoided but mainly to follow and validate those predictions experimentally by achieving the successful VIG sample [21, 14]. A careful consideration need to be made when reproducing the VIG construction for larger size and the use of tempered glass could be used and to evaluate the applicability of the obtained results to samples of larger size, current findings are limited to smaller size VIG such as the dimensions of 300mm·300mm·4mm or 500mm·500mm·4mm.

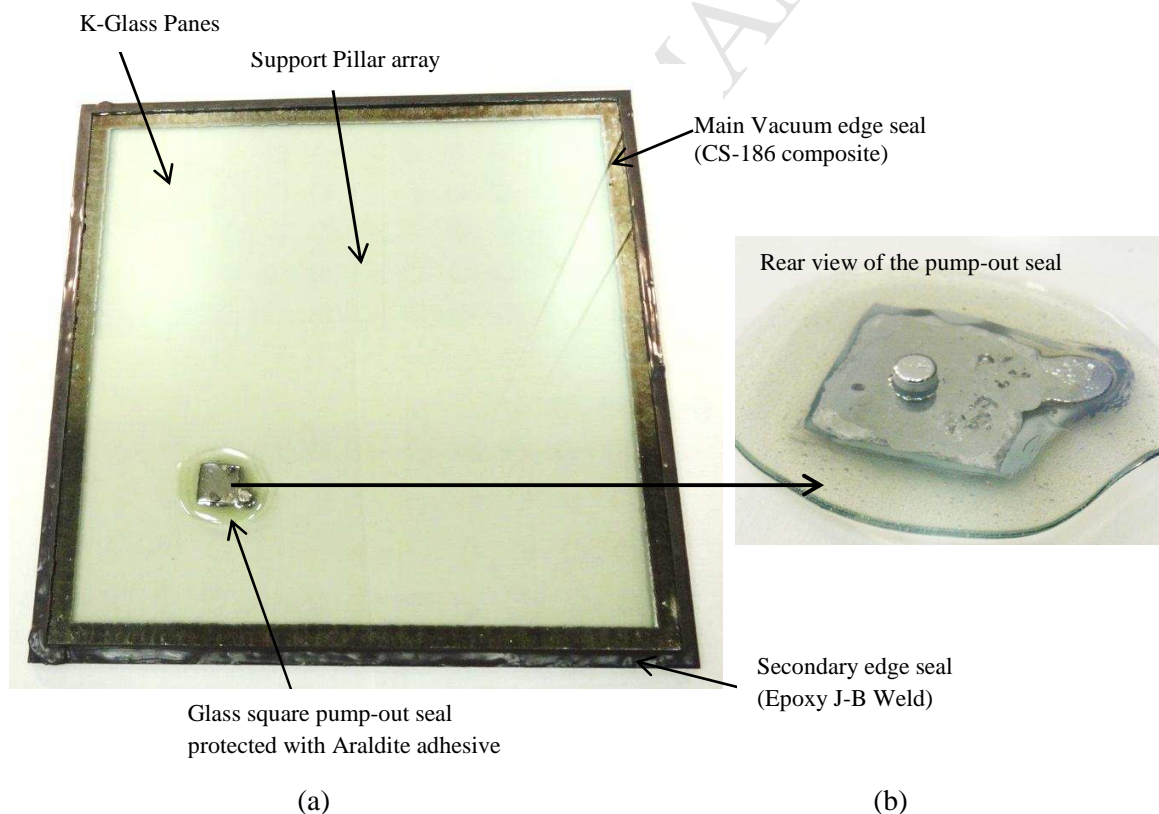


Fig. 12. (a) An improved VIG sample, made of 300mm·300mm·4mm in size, showing the main edge seal 10 mm wide made of CS-186 composite and a support edge seal, 4 mm wide, made of steel reinforced epoxy and (b) the pump-out hole made of the aforementioned composite protected with Araldite adhesive.

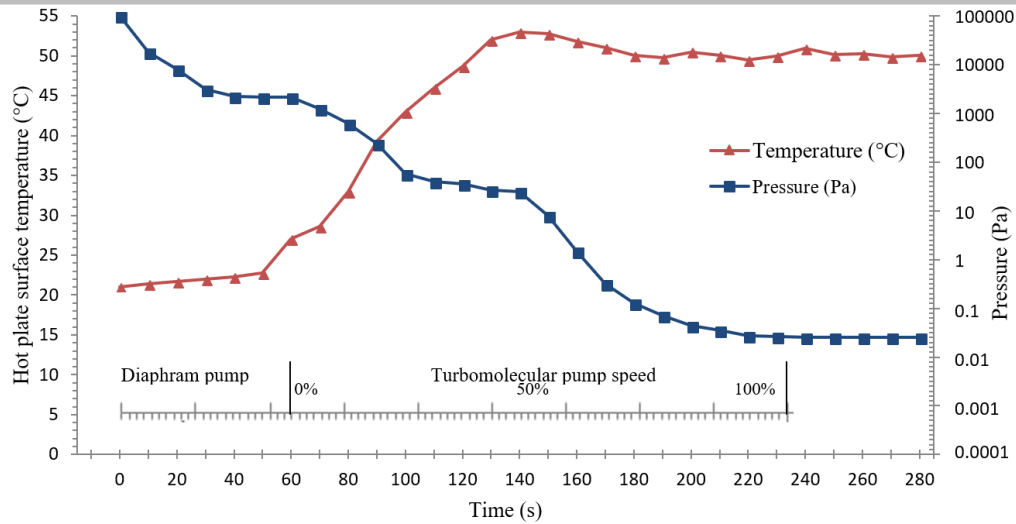


Fig. 13. The experimental temperature/pressure regimes of sample shown in Fig 12, in which a vacuum pressure of 0.042 Pa at 50°C was achieved with the successful pump-out hole seal without any leak to the edge sealing area.

6. Thermal performance analyses of the VIG

6.1. Validated finite volume modelling approach

An experimentally and theoretically validated finite volume model (FVM) of Fang et al.(2005) [31]; Fang et al.(2006) [15] and Fang et al. (2009) was utilised for the thermal performance analyses of VIG, size of 300mm·300mm·4mm rebated by 10 mm in a solid wood frame and 10 mm main edge seal. The details of the analytical model are reported in Fang et al. (2006) [22]. A validated set of equations, including the direct depiction of the support pillars incorporated to the FVM, were solved for the fabricated design of VIG at the cavity vacuum pressure of 0.042 Pa. The reason to model only one quarter of the VIG is the symmetrical geometry of the whole sample of VIG under the ISO ambient conditions [41] representing the complete thermal performance. As per ISO (2000) [41] standard, the average air temperatures of the cold and warm sides of the glass panes are set to be 20°C and 0°C, respectively. The inside and outside surface heat transfer coefficients are $7.7 \text{ W m}^{-2}\text{K}^{-1}$ and $25 \text{ W m}^{-2}\text{K}^{-1}$, respectively. The cylindrical nature of support pillars in FVM is represented as a cube, with square base, support pillar (length of $\sqrt{\pi a}$) having equivalent area utilised that conduct the same amount of heat transfer which is a validated approach of Fang et al. (2009) [22]. A higher density of nodes were utilised in the mesh that represents each support pillar to allow maximum possible levels of accuracy in the calculation of heat transfer and again the accuracy is validated in Fang et al. (2005) and the approach is comparable with the results of Wilson et al. (1998) [16] and Collins and Robinsons (1991) [19]. Initial tests of this FVM were performed with the 50·50 nodes distributed on the y and z directions on the glazing surface and with 20 nodes on the x direction. The thermal transmittance at the centre-of-pane for the indium based vacuum glazing with emittance of 0.03 was determined to be $0.36 \text{ W m}^{-2}\text{K}^{-1}$ with a glass pane thickness of 6 mm. It was found identical with the findings of Griffiths et al. (1998) [13] thus this modelling approach is suitable to simulate a practical heat flow with high accuracy of predicting the thermal transmittance of VIG based on the achievable cavity vacuum pressure of 0.042 Pa. The boundary conditions implemented in the finite-volume model of the VIG are listed in Table 2.

Table 2

Boundary conditions implemented in the validated finite-volume model of the VIG.

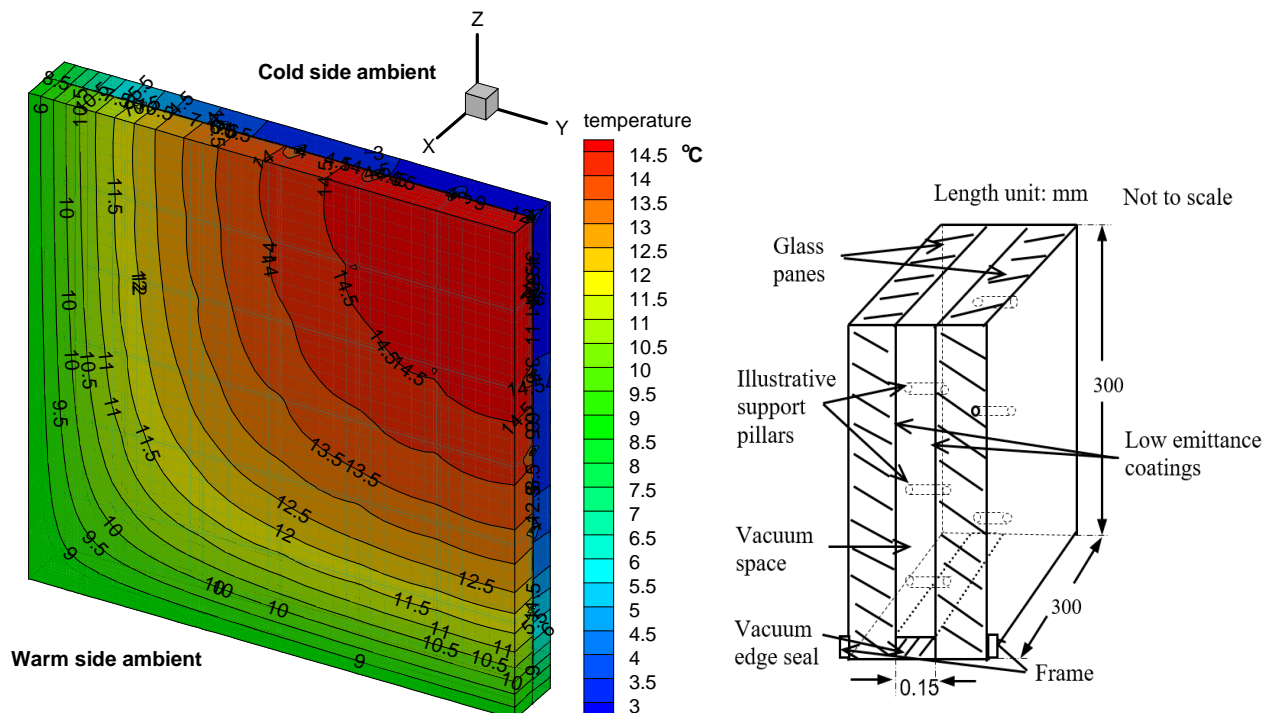
Constructional element	Property	Value and/or material type
Main edge seal	Material	CS186 composite
	Width	10 mm [‡]
	Thermal conductivity	46.49 Wm ⁻¹ K ⁻¹ *
Glass pane (Pilkington K type)	Thermal conductivity	1 Wm ⁻¹ K ⁻¹
Emittance	Three surfaces (Hard coating)	0.15/tin-oxide [‡]
Frame (wood)	Thermal conductivity	0.138 Wm ⁻¹ K ⁻¹
Support pillar	Material	Stainless steel 304
	Diameter	0.3 mm
	Height	0.15 mm
	Pillar separation	24 mm
	Thermal conductivity	16.2 Wm ⁻¹ K ⁻¹

*Measured thermal conductivities are reported by Memon (2017) [30].

[‡] In the analyses the comparison is also presented by varying the emittance and edge seal on the thermal performance of VIG

6.2. Thermal performance of the VIG

The centre-of-pane (U_{centre}) and total thermal transmittance (U_{total}) values of the VIG predicted to be 0.91 Wm⁻²K⁻¹ and 1.05 Wm⁻²K⁻¹, respectively. Isotherms of the cold and warm side of the VIG are presented in Fig. 14a. This is compared with [28] predictions based on an indium sealed vacuum glazing sample dimensions of 400mm·400mm·4mm with SnO₂ coatings on the inner surface of two glass sheets with a pillar spacing of 25 mm, the U_{centre} and U_{total} values were reported to be 1 and 1.19 Wm⁻²K⁻¹, respectively. A decrease of U_{centre} (0.09 Wm⁻²K⁻¹) and U_{total} (0.14 Wm⁻²K⁻¹) values were predicted due to the use of a 10 mm rebated frame depth and the 10 mm main edge seal covered inside the frame as shown in Fig. 14b. Although the wider layer of edge seal caused increased edge-effects, which results in higher thermal transmittance values of the glazing. The total heat transfer can be reduced by reducing the edge seal width and emissivity of the coatings on the inner surfaces of VIG. For example, a 6mm wide indium edge sealed vacuum glazing was predicted to have U_{total} and U_{centre} values of 0.9 Wm⁻²K⁻¹ and 0.36 Wm⁻²K⁻¹, respectively, using soft low emittance coatings [13].



(a)

(b)

Fig. 14. (a) isotherms of the one quarter of the VIG where the thickness along the x axial direction is enlarged by factor of 2.5 compared to the length in y and z direction showing the temperature distribution from the vacuum edge seal towards the centre-of-pane glazing area. (a) Schematic diagram of the modelled VIG

6.3. An influence of reducing the width of vacuum edge seal and the emittance of inner surface coatings on the thermal performance of VIG.

Fig. 15 shows, that for the VIG size of 300mm·300mm·4mm with an emittance of 0.15, when the edge seal width decreased from 10 mm to 3 mm then the U_{centre} and U_{total} values also decreased from 0.91 $\text{Wm}^{-2}\text{K}^{-1}$ and 1.05 $\text{Wm}^{-2}\text{K}^{-1}$ to 0.81 $\text{Wm}^{-2}\text{K}^{-1}$ (an improvement of 11.0%) and 0.91 $\text{Wm}^{-2}\text{K}^{-1}$ (an improvement of 13.3%) respectively. For the aforementioned size of VIG with an emittance of 0.03, similar decrement of the edge seal from 10 mm to 3 mm further improved the U_{centre} and U_{total} values from 0.71 $\text{Wm}^{-2}\text{K}^{-1}$ and 0.84 $\text{Wm}^{-2}\text{K}^{-1}$ to 0.62 $\text{Wm}^{-2}\text{K}^{-1}$ (an improvement of 12.7.0%) and 0.71 $\text{Wm}^{-2}\text{K}^{-1}$ (an improvement of 15.5%) respectively. These results indicate that further work on reducing the main edge seal width would improve the thermal transmittance but experimentally reducing the edge seal width has not been possible as it compromises the integrity and hermeticity of the edge seal of VIG. However, the low-e coatings, such as silver thin films or transparent nano-structured thin films, could replace SnO_2 coating on K glass as it improves the thermal transmittances of VIG.

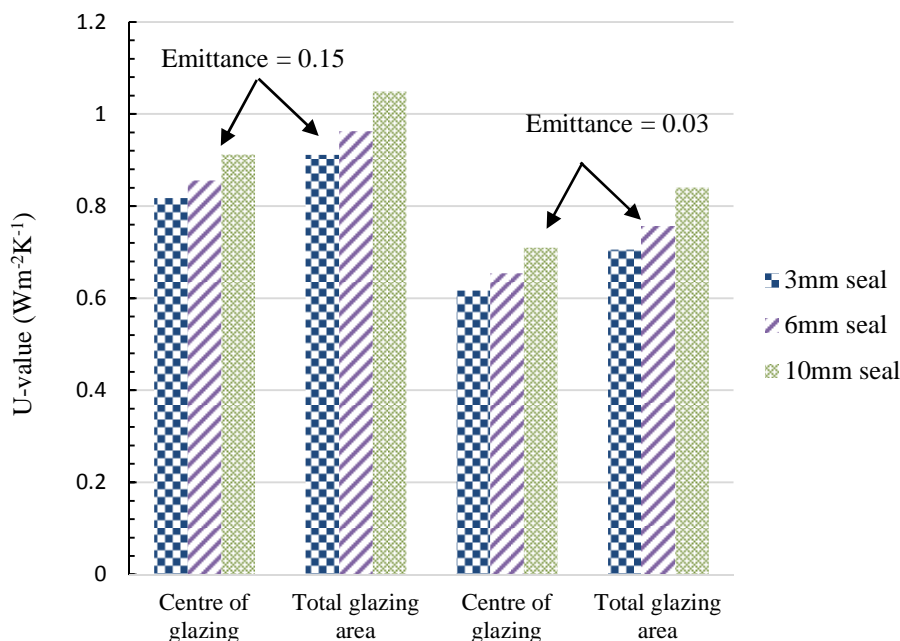


Fig. 15. Predicted U-value at the centre of glazing and total glazing areas of the 0.3 m by 0.3 m vacuum glazing with edge seal with of 3 mm, 6 mm and 10 mm.

6.4. An influence of increasing the size and reducing the width of vacuum edge seal on the thermal performance of VIG.

Fig. 16 shows, when the glazing size increased from 300mm·300mm·4mm to 400mm·400mm·4mm with 10 mm edge seal, the U_{centre} and U_{total} values decreased from $0.91 \text{ Wm}^{-2}\text{K}^{-1}$ and $1.05 \text{ Wm}^{-2}\text{K}^{-1}$ to $0.86 \text{ Wm}^{-2}\text{K}^{-1}$ (an improvement of 4.4%) and $0.96 \text{ Wm}^{-2}\text{K}^{-1}$ (an improvement of 8.6%) respectively. For the VIG with 3 mm wide edge seal, the U_{centre} and U_{total} values decreased from $0.81 \text{ Wm}^{-2}\text{K}^{-1}$ and $0.91 \text{ Wm}^{-2}\text{K}^{-1}$ to $0.79 \text{ Wm}^{-2}\text{K}^{-1}$ (an improvement of 2.5%) and $0.86 \text{ Wm}^{-2}\text{K}^{-1}$ (an improvement of 5.5%) respectively. These results indicate that larger the glazing size the lower the thermal transmittance values. Whilst with a wider edge seal, because of its edge effects, the thermal transmittance values are larger than that of the glazing with a narrower edge seal. As same as with other kind of edge seal, a larger sized vacuum glazing will provide better thermal performance compared to the one with small size.

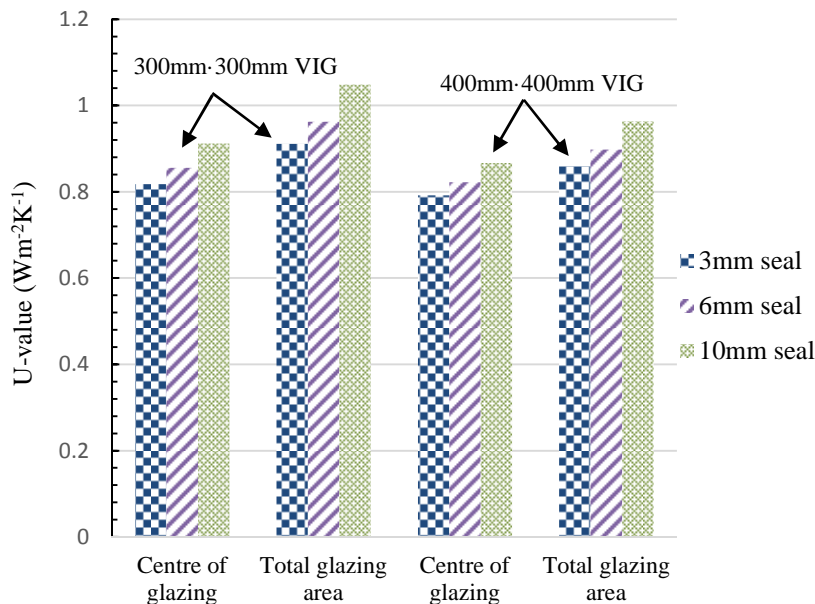


Fig. 16. Predicted U-value at the centre of glazing and total glazing areas of the 300mm·300mm and 400mm·400mm VIG with edge seal width of 3 mm, 6 mm and 10 mm.

7. Conclusions

Hermeticity of vacuum edge-seal has been the paramount requirement, specifically, in the evolution of smart windows. In this paper, a composite ($\text{Sn}_{56}\text{Pb}_{39}\text{Zn}_3\text{Sb}_1$ - AlTiSiCu_1 wt%) edge-sealed vacuum insulated glazing successfully developed. The main conclusions are summarised into the following four features:

- (1) A high-vacuum glazing fabrication system, successfully designed and constructed, achieved $4.35 \cdot 10^{-5}$ Pa with a modified vacuum cup; this proved to reduce the risk of dislocation of the heating block and the degradation of Viton O rings due to unwavering heating required for sealing the pump-out hole with glass square inside the vacuum pump during evacuation.

(2) The microstructural investigations, using FIB-SEM and X-ray CT, of $\text{Sn}_{56}\text{Pb}_{39}\text{Zn}_3\text{Sb}_1\text{-AlTiSiCu}_1$ wt% composite showed negligible traces of micro voids with trapped air inside, when sealed with k-glass, and homogeneity, when ultrasonically soldered on the glass surface at the vibration frequency of 25-30 kHz with the tip set-point at 190°C. It led to the development of new methods for the formation of vacuum edge-seal.

(3) Experimental investigations of the seven fabricated VIG samples, each of size 300mm·300mm·4 mm, showed that increasing the hot-plate surface temperatures improved the cavity vacuum pressure whilst expediting the pump-out hole sealing process but also increases temperature induced stresses. Successful pump-out hole sealing process of VIG attained at the hot-plate set-point temperature of 50°C and the approximate cavity pressure of 0.042 Pa. More than five similar samples of this process having different sizes fabricated verifies the recurrent sealing of the pump-out hole and cavity vacuum pressure. The experimental observations show repetitive behaviour of stress patterns across the support pillars indicated a vacuum-tight edge seal. one of the vital issue in VIG is its durability and its ageing but in this paper the hermeticity of the composite edge seal itself was analysed by analysing the evacuation time in achieving and maintaining the cavity vacuum pressure before and after evacuation whilst analysing the surface temperature induction influence on vacuum pressure. The durability of the whole sample of VIG itself is significantly important and is a dynamic issue because, despite of successful constructions of VIG, there is always an uncertainty of the degradation of the cavity vacuum pressure because of some gas molecules may remained in the cavity that react when exposed to sunlight and/or under extreme climate conditions for longer time (e.g. after 10 years) due to the development of CO inside the cavity that degrades the vacuum layer. It is apparent that VIG will be exposed to sunlight and need to be designed to sustain at different climate temperatures and for over 20 years in order to avoid degradation of vacuum. For this the future work recommendation to tackle this issue is to utilise non-evaporable getters in VIG and perform ageing tests.

(4) A validated finite volume model, incorporating support pillars, employed and calculated the U_{centre} and U_{total} values of $0.91 \text{ Wm}^{-2}\text{K}^{-1}$ and $1.05 \text{ Wm}^{-2}\text{K}^{-1}$ respectively for the fabricated VIG sample (size of 300mm·300mm·4mm) rebated by 10 mm in a solid wood frame at the cavity vacuum pressure of 0.042 Pa. Improvements of 11 % ($0.81 \text{ Wm}^{-2}\text{K}^{-1}$) and 13.3% ($0.91 \text{ Wm}^{-2}\text{K}^{-1}$) in the U_{centre} and U_{total} values can be achieved by reducing the vacuum edge-seal width from 10 mm to 3 mm at the surface coating emittance of 0.15. For the same size VIG with an emittance of 0.03, when the width of the edge seal decreased from 10 mm to 3 mm the U_{centre} and U_{total} values were predicted to be from $0.71 \text{ Wm}^{-2}\text{K}^{-1}$ and $0.84 \text{ Wm}^{-2}\text{K}^{-1}$ to $0.62 \text{ Wm}^{-2}\text{K}^{-1}$ (an improvement of 12.7.0%) and $0.71 \text{ Wm}^{-2}\text{K}^{-1}$ (an improvement of 15.5%) respectively. This result indicates that further work on reducing the main edge seal width would improve the thermal transmittance values but experimentally reducing the edge seal width has not been possible as it compromises the durability of the edge seal of VIG. However, the low-e coatings, such as silver thin films or transparent nano-structured thin films, could replace SnO_2 coating on K glass as it improved the thermal transmittances of VIG and is suitable for this type of vacuum edge seal.

Acknowledgement

This work was supported by the Engineering and Physical Sciences Research Council (EPSRC) of the UK (EP/G000387/1).

References

- [1]. Memon, S., 2014. Analysing the potential of retrofitting ultra-low heat loss triple vacuum glazed windows to an existing UK solid wall dwelling. *International Journal of Renewable Energy Development*, 3(3), p.161.
- [2]. Moss, R.W., Shire, G.S.F., Eames, P.C., Henshall, P., Hyde, T. and Arya, F., 2018a. Design and commissioning of a virtual image solar simulator for testing thermal collectors. *Solar Energy*, 159, pp.234-242.
- [3]. Moss, R.W., Henshall, P., Arya, F., Shire, G.S.F., Hyde, T. and Eames, P.C., 2018b. Performance and operational effectiveness of evacuated flat plate solar collectors compared with conventional thermal, PVT and PV panels. *Applied Energy*, 216, pp.588-601.
- [4]. Eames, P.C., 2008. Vacuum glazing: current performance and future prospects. *Vacuum*, 82(7), pp.717-722.
- [5]. Memon, S., Farukh, F., Eames, P.C. and Silberschmidt, V.V., 2015. A new low-temperature hermetic composite edge seal for the fabrication of triple vacuum glazing. *Vacuum*, 120, pp.73-82.
- [6]. Memon, S. and Eames, P.C., 2017. Predicting the solar energy and space-heating energy performance for solid-wall detached house retrofitted with the composite edge-sealed triple vacuum glazing. *Energy Procedia*, 122, pp.565-570.
- [7]. Allen, K., Connelly, K., Rutherford, P. and Wu, Y., 2017. Smart windows—Dynamic control of building energy performance. *Energy and Buildings*, 139, pp.535-546.
- [8]. Wu, L.Y., Zhao, Q., Huang, H. and Lim, R.J., 2017. Sol-gel based photochromic coating for solar responsive smart window. *Surface and Coatings Technology*, 320, pp.601-607.
- [9]. Manz, H., Brunner, S. and Wulschleger, L., 2006. Triple vacuum glazing: Heat transfer and basic mechanical design constraints. *Solar Energy*, 80(12), pp.1632-1642.
- [10]. Baetens, R., Jelle, P. Gustavsen, A. 2011. Aerogel insulation for building applications: A state of the art review. *Energy and Buildings*, 43, pp 761-769.
- [11]. Weston, G.F., 2013. *Ultrahigh vacuum practice*. Elsevier.
- [12]. Collins, R.E. and Simko, T.M., 1998. Current status of the science and technology of vacuum glazing. *Solar Energy*, 62(3), pp.189-213.
- [13]. Griffiths, P.W., di Leo, M., Cartwright, P., Eames, P.C., Yianoulis, P., Leftheriotis, G. and Norton, B., 1998. Fabrication of evacuated glazing at low temperature. *Solar Energy*, 63(4), pp.243-249.
- [14]. Fischer-Cripps, A.C., Collins, R.E., Turner, G.M. and Bezzel, E., 1995. Stresses and fracture probability in evacuated glazing. *Building and environment*, 30(1), pp.41-59.
- [15]. Fang, Y., Eames, P.C., Norton, B. and Hyde, T.J., 2006. Experimental validation of a numerical model for heat transfer in vacuum glazing. *Solar Energy*, 80(5), pp.564-577.
- [16]. Wilson, C.F., Simko, T.M. and Collins, R.E., 1998. Heat conduction through the support pillars in vacuum glazing. *Solar Energy*, 63(6), pp.393-406.
- [17]. Koebel, M.M., Manz, H., Mayerhofer, K.E. and Keller, B., 2010. Service-life limitations in vacuum glazing: A transient pressure balance model. *Solar Energy Materials and Solar Cells*, 94(6), pp.1015-1024.
- [18]. [dataset] Memon, S. 2013. Design, Fabrication and Performance Analysis of Vacuum Glazing Units Fabricated with Low and High Temperature Hermetic Glass Edge Sealing Materials. PhD Thesis. Loughborough University: UK. DOI: <https://dspace.lboro.ac.uk/2134/14562>.
- [19]. Collins, R.E. and Robinson, S.J., 1991. Evacuated glazing. *Solar Energy*, 47(1), pp.27-38.

- [20]. Benson, D.K., Tracy, C.E. and Jorgensen, G.J., 1984, November. Laser sealed evacuated window glazings. In *Optical Materials Technology for Energy Efficiency and Solar Energy Conversion III* (Vol. 502, pp. 146-152). International Society for Optics and Photonics.
- [21]. Wang, J., Eames, P.C., Zhao, J.F., Hyde, T. and Fang, Y., 2007. Stresses in vacuum glazing fabricated at low temperature. *Solar energy materials and solar cells*, 91(4), pp.290-303.
- [22]. Fang, Y., Hyde, T., Hewitt, N., Eames, P.C. and Norton, B., 2009. Comparison of vacuum glazing thermal performance predicted using two-and three-dimensional models and their experimental validation. *Solar Energy Materials and Solar Cells*, 93(9), pp.1492-1498.
- [23]. Robinson, S.J. and Collins, R.E., 1989, September. Evacuated windows-theory and practice. In *ISES solar world congress, international solar energy society, Kobe, Japan*.
- [24]. Collins, R.E., Fischer-Cripps, A.C. and Tang, J.Z., 1992. Transparent evacuated insulation. *Solar Energy*, 49(5), pp.333-350.
- [25]. Garrison, J.D. and Collins, R.E., 1995. Manufacture and cost of vacuum glazing. *Solar Energy*, 55(3), pp.151-161.
- [26]. Uhlmann, D. ed., 2012. *Elasticity and Strength in Glasses: Glass: Science and Technology* (Vol. 5). Elsevier.
- [27]. Griffiths, P.W., Eames, P.C., Hyde, T.J., Fang, Y. and Norton, B., 2006. Experimental characterization and detailed performance prediction of a vacuum glazing system fabricated with a low temperature metal edge seal, using a validated computer model. *Journal of solar energy engineering*, 128(2), pp.199-203.
- [28]. Zhao, J.F., Eames, P.C., Hyde, T.J., Fang, Y. and Wang, J., 2007. A modified pump-out technique used for fabrication of low temperature metal sealed vacuum glazing. *Solar Energy*, 81(9), pp.1072-1077.
- [29]. Fang, Y., Hyde, T.J., Arya, F., Hewitt, N., Eames, P.C., Norton, B. and Miller, S., 2014. Indium alloy-sealed vacuum glazing development and context. *Renewable and Sustainable Energy Reviews*, 37, pp.480-501.
- [30]. Memon, S., 2017. Experimental measurement of hermetic edge seal's thermal conductivity for the thermal transmittance prediction of triple vacuum glazing. *Case studies in thermal engineering*, 10, pp.169-178.
- [31]. Fang, Y., Eames, P.C., Hyde, T.J. and Norton, B., 2005. Complex multimaterial insulating frames for windows with evacuated glazing. *Solar energy*, 79(3), pp.245-261.
- [32]. Wilfert, S. and Edelmann, C., 2004. Miniaturized vacuum gauges. *Journal of Vacuum Science & Technology A: Vacuum, Surfaces, and Films*, 22(2), pp.309-320.
- [33]. Dennis, N.T.M. and Heppell, T.A., 1968. *Vacuum system design*. Chapman and Hall Ltd, London.
- [34]. Guthrie, A. 1963. *Vacuum Technology*. John Wiley and Sons, Inc, New York.
- [35]. Kohl, W.H., 1967. *Handbook of Materials and Techniques for Vacuum Devices*, Reinhold Pub. Co., New York.
- [36]. Corruccini, R.J., 1959. Gaseous heat conduction at low pressures and temperatures. *Vacuum*, 7, pp.19-29.
- [37]. Turnbull, A.H., Barton, R.S. and Rivière, J.C., 1964. An introduction to vacuum technique. *American Journal of Physics*, 32(8), pp.649-649.
- [38]. Simko, T.M., Fischer-Cripps, A.C. and Collins, R.E., 1998. Temperature-induced stresses in vacuum glazing: Modelling and experimental validation. *Solar energy*, 63(1), pp.1-21.
- [39]. Lenzen, M. and Collins, R.E., 1997. Long-term field tests of vacuum glazing. *Solar Energy*, 61(1), pp.11-15.

- 1 [40]. Wullschleger, L., Manz, H. and Wakili, K.G., 2009. Finite element analysis of temperature-induced
2 deflection of vacuum glazing. *Construction and Building Materials*, 23(3), pp.1378-1388.
- 3 [41]. ISO, 2000. ISO 9050 Glass in building – Determination of light transmittance, solar direct
4 transmittance, total solar energy transmittance and ultraviolet transmittance, and related glazing
5 factors. Geneva, Switzerland.
6

Highlights

- Novel design and construction of vacuum insulated glazing (VIG) were discussed.
- A vacuum edge-seal made of composite ($\text{Sn}_{56}\text{Pb}_{39}\text{Zn}_3\text{Sb}_1$ - AlTiSiCu_1 wt%) was analyzed.
- Influences of temperatures on evacuation and pump-out sealing of VIG were studied.
- A high-vacuum pressure of 0.042 Pa at 50°C surface temperature was achieved with VIG.
- Thermal performance of VIG with surface-coatings and vacuum-edge seal was analysed.